
Exact Fixed-Point Constraints in Neural-ODEs with Provable Universality

Feliciano Giuseppe Pacifico^{1,2}
felicianogiuseppe.pacifico@phd.unipi.it

Duccio Fanelli² Lorenzo Buffoni²

Lorenzo Chicchi²

Diego Febbe²

Raffaele Marino²

¹Department of Informatics and Computer Science, University of Pisa, Italy

²Department of Physics and Astronomy and INFN, University of Florence, Sesto Fiorentino, Italy

Abstract

We introduce a technique that enables Neural-ODEs to approximate arbitrary velocity fields with a priori planted fixed-points. Specifically, a recipe is given to explicitly accommodate for a finite collection of points in the reference multi-dimensional space of the Neural-ODE where the velocity field is exactly equal to zero. In this way, the gradient-based training is rigorously constrained inside the prescribed hypothesis class while leaving the expressive power of the Neural-ODE unaltered. We rigorously prove the universality of the Neural-ODE under any local constraints in the velocity field and give a computationally convenient way of imposing the fixed points. Our method is then tested on two paradigmatic physical models.

1 Introduction

Neural ordinary differential equations (Neural-ODEs) Chen et al. [2018] define a class of deep learning models that seek at representing neural network layers as a continuous-time system. Instead of a discrete sequence of hidden layers, a Neural-ODE parameterizes the derivative of the state vector via a neural network. Concretely, the forward pass materializes as the evolution of a point in a multi-dimensional space through a system of coupled ordinary differential equations, written in terms of a deep neural network which bears universality traits Teshima et al. [2020], Ishikawa et al. [2023].

Hard-constrained neural architectures have been investigated from several complementary viewpoints. Classical contributions addressed exact interpolation and constrained approximation in feed-forward networks Min and Azizan [2024], Cao et al. [2010], while seminal and recent works in the PINN literature exploited constraint-preserving ansatz, distance functions, and hard linear equality constraints to impose boundary or algebraic conditions exactly Lagaris et al. [1998], Chen et al. [2024], Sukumar and Srivastava [2022]. Non-trivial hard constraints can be also enforced without losing universal approximation guarantees Constantinescu and Popescu [2023]. For continuous-depth models, related ideas have been explored in several directions, including manifold-constrained Neural-ODEs with universality results Elamvazhuthi et al. [2023] and stability-oriented Neural-ODE constructions based on Lyapunov-stable equilibria Kang et al. [2021]. Exact feasibility has been also enforced via differentiable optimization layers Amos and Kolter [2017]. More recently, dedicated methods have been proposed to constrain the learned dynamics Gagliani et al. [2026], Chicchi et al. [2025] via spectral decomposition and orthogonal projection operators. Other approaches assume projecting the vector field onto the tangent space of a constraint manifold White et al. [2024]. These results imply that structural priors and exact constraints can be embedded into trainable architectures in a principled way.

Yet, the specific issue of prescribing beforehand a finite collection of exact fixed points in a Neural-ODE velocity field, while retaining universality within the class of compatible target dynamics, is still an open question that remains unanswered despite the above mentioned constructions. Planted-fixed-point could on the one side contribute to enhance the model interpretability, as learning takes place within a limpid dynamical framework; on the other hand, the resulting architecture might, at least in principle, lose expressive power precisely because of the imposed equilibrium constraints.

The goal of this work is to bridge the above viewpoints by using a Neural-ODE which accommodates beforehand for a finite set of planted fixed points, via a suitably tailored parameterization, while keeping the remaining parameters free to fit any arbitrary compatible dynamics, thus retaining universality. The paper is organized as follows. Section 2 defines the problem, while Section 3 presents the proof of the main theorem establishing the universality of the proposed approach. In Section 4 we will turn to discussing the generalized procedure to enforce the fixed-points in the generated velocity fields. Vector field regression for models with planted fixed-points will be demonstrated in Section 5.

2 Stating the problem

Consider a Neural-ODE model that we generally formulate as:

$$\dot{x} = Af(Bx + b) \equiv F_\theta(x) \quad (1)$$

where $A \in \mathbb{R}^{n \times m}$, $B \in \mathbb{R}^{m \times n}$, $b \in \mathbb{R}^m$, $f(\cdot)$ is a proper non-linear function. The multi-layer perceptron that defines the velocity field of the above Neural-ODE is denoted by $F_\theta(x)$ in short, where θ stands for the cumulative set of free tunable parameters. Imagine that a procedure exists to insert in the above vector field $F_\theta(x)$ a set of C fixed-point constraints, namely:

$$F_\theta(\bar{x}^{(l)}) = 0, \quad l = 1, \dots, C \quad (2)$$

The specific procedure that we have devised to enforce these constraints, will be illustrated in Section 4.

Given the above, a natural question arises: does imposing hard equilibrium constraints reduce the expressive power of the Neural-ODE vector field? This is the question that we set to answer in the forthcoming Section. More specifically, we will prove that, on compact sets, the family of vector fields depictable by a one-hidden-layer Neural-ODE remains a universal approximator, even when restricted to the subclass satisfying the prescribed constraints. Equivalently, the constrained parametrizations do not merely enforce a local condition on the vector field: they do so without sacrificing universality within the class of target dynamics that share the same constraints.

3 Universality under local constraints

Unlike other literature dealing with hard-constrained architecture Min and Azizan [2024], Lagaris et al. [1998], Cao et al. [2010], Chen et al. [2024], Constantinescu and Popescu [2023], Sukumar and Srivastava [2022], in this work, the hard constraints are used to prescribe fixed points of the Neural-ODE vector field. The theorem below shows that these exact equilibrium constraints do not destroy the approximation power of the model class: the constrained family remains dense in the class of continuous vector fields vanishing at the prescribed points. We are not aware of a previous proof of this exact statement in the present setting and based on the constructive correction argument used here.

Theorem 1 (Universal approximation with prescribed fixed points via kernel constraints). *Let $K \subset \mathbb{R}^n$ be compact and let $\bar{x}^{(1)}, \dots, \bar{x}^{(C)} \in K$ be distinct. Let $\sigma : \mathbb{R} \rightarrow \mathbb{R}$ be a continuous activation with two distinct one-sided limits*

$$\alpha := \lim_{t \rightarrow -\infty} \sigma(t), \quad \beta := \lim_{t \rightarrow +\infty} \sigma(t), \quad \alpha \neq \beta.$$

and define $f : \mathbb{R}^m \rightarrow \mathbb{R}^m$ component-wise by $(f(z))_j = \sigma(z_j)$.

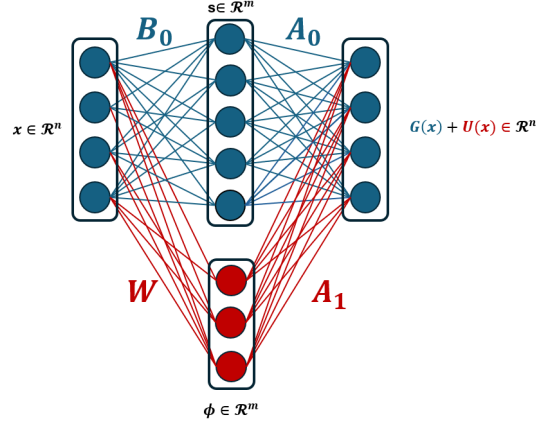


Figure 1: A schematic layout of the architectural construction employed in the proof of the Theorem.

Consider the network class (vector fields)

$$\mathcal{N}_m := \left\{ F_\theta(x) = Af(Bx + b) : A \in \mathbb{R}^{n \times m}, B \in \mathbb{R}^{m \times n}, b \in \mathbb{R}^m \right\}.$$

Define the constrained target class

$$\mathcal{F}_0 := \left\{ F \in C(K, \mathbb{R}^n) : F(\bar{x}^{(l)}) = 0 \forall l = 1, \dots, C \right\}.$$

Then, for every $F \in \mathcal{F}_0$ and every $\varepsilon > 0$, there exists an integer m and parameters (A, B, b) such that

1. $F_\theta(\bar{x}^{(l)}) = 0$ for all $l = 1, \dots, C$ (exact fixed points),
2. $\sup_{x \in K} \|F(x) - F_\theta(x)\| < \varepsilon$.

Equivalently: the constrained network class

$$\mathcal{N}_{m,0} := \{F_\theta \in \mathcal{N}_m : F_\theta(\bar{x}^{(l)}) = 0 \forall l\}$$

is dense in \mathcal{F}_0 in the uniform norm.

Proof. Step 0 (Fixed points are hidden vectors in the kernel of A). For any (A, B, b) and any $x \in K$,

$$F_\theta(x) = Af(Bx + b).$$

Thus for each planted point $\bar{x}^{(l)}$,

$$F_\theta(\bar{x}^{(l)}) = 0 \iff A s_l = 0, \quad s_l := f(B\bar{x}^{(l)} + b) \in \mathbb{R}^m.$$

So the fixed-point constraints are equivalent to requiring

$$s_l \in \ker(A) \quad \forall l.$$

Notice that no orthogonality is needed for the above conclusion to hold. The practical procedure to enforce s_l in the kernel of A will be addressed in Section 4.

Step 1 (Unconstrained approximation). Let $F \in \mathcal{F}_0$ and $\varepsilon > 0$ be given.

By the canonical universal approximation theorem Hornik et al. [1989], Cybenko [1989] for one-hidden-layer networks (vector-valued version obtained component-wise), there exist m_0 and (A_0, B_0, b_0) such that

$$G(x) := A_0 f(B_0 x + b_0)$$

satisfies

$$\sup_{x \in K} \|F(x) - G(x)\| < \delta,$$

where $\delta > 0$ will be chosen later.

Since $F(\bar{x}^{(l)}) = 0$ for all l , we get the pointwise bound

$$\|G(\bar{x}^{(l)})\| = \|G(\bar{x}^{(l)}) - F(\bar{x}^{(l)})\| < \delta \quad \forall l.$$

Define the residual vectors

$$r_l := -G(\bar{x}^{(l)}) \in \mathbb{R}^n, \quad R := [r_1, \dots, r_C] \in \mathbb{R}^{n \times C}.$$

Then $\|r_l\| < \delta$ for all l .

Step 2 (Choose C extra hidden units with an invertible evaluation matrix). We will add C extra hidden nodes, going from m_0 to $m_0 + C$ elements. For $k = 1, \dots, C$, choose parameters $(w_k, \beta_k) \in \mathbb{R}^n \times \mathbb{R}$ and define scalar features (see schematic layout 1)

$$\phi_k(x) := \sigma(w_k^\top x + \beta_k).$$

Let $\phi(x) = (\phi_1(x), \dots, \phi_C(x))^\top \in \mathbb{R}^C$ and define the evaluation matrix $M \in \mathbb{R}^{C \times C}$ by

$$M_{lk} := \phi_k(\bar{x}^{(l)}).$$

As proven in Appendix A, it exists a choice of $\{(w_k, \beta_k)\}_{k=1}^C$ such that M is invertible.

Step 3 (Construct a corrected interpolant network that enforces the sought constraints exactly). Define an $n \times C$ output weight matrix A_1 as the unique solution of

$$A_1 M^\top = R.$$

Since M is invertible (see Appendix A), this solution exists and is

$$A_1 = R(M^\top)^{-1}.$$

Define the correction $U(x)$ to the output component (that is needed to enforce the imposed constraints) as

$$U(x) := A_1 \phi(x) \in \mathbb{R}^n.$$

Now evaluate at the planted points $\bar{x}^{(l)}$. Note that $\phi(\bar{x}^{(l)}) = M_{l,:}^\top$. Hence

$$U(\bar{x}^{(l)}) = A_1 \phi(\bar{x}^{(l)}) = A_1 M_{l,:}^\top = (A_1 M^\top) e_l = R e_l = r_l = -G(\bar{x}^{(l)}).$$

where e_l stands for the l -th element of the canonical basis. Therefore, the corrected output function reads

$$H(x) := G(x) + U(x)$$

and satisfies

$$H(\bar{x}^{(l)}) = G(\bar{x}^{(l)}) + U(\bar{x}^{(l)}) = 0 \quad \forall l.$$

So H satisfies the fixed-point constraints exactly.

Also note that H is still a one-hidden-layer network: it is the sum of two one-hidden-layer networks, which is again a one-hidden-layer network after concatenating hidden units. Concretely, define $m = m_0 + C$, where C is the total number of imposed constraints and set

$$B := \begin{bmatrix} B_0 \\ W \end{bmatrix}, \quad b := \begin{bmatrix} b_0 \\ \beta \end{bmatrix}, \quad A := [A_0 \quad A_1],$$

where W has rows w_k^\top and $\beta = (\beta_1, \dots, \beta_C)^\top$. Then indeed

$$H(x) = Af(Bx + b).$$

Thus $H \in \mathcal{N}_m$ and $H(\bar{x}^{(l)}) = 0 \forall l$, i.e. $H \in \mathcal{N}_{m,0}$.

Notice that, by Step 0, for this constructed A, B, b we automatically have

$$s_l = f(B\bar{x}^{(l)} + b) \in \ker(A),$$

Step 4 (Uniform error control). We estimate the approximation error:

$$\sup_{x \in K} \|F(x) - H(x)\| \leq \sup_{x \in K} \|F(x) - G(x)\| + \sup_{x \in K} \|U(x)\|.$$

The first term is $< \delta$ by Step 1.

For the second term, by the hypothesis on σ , it is bounded on \mathbb{R} . This holds for key non linear functions such as, tanh and sigmoid. Then there exists a constant M_σ such that $|\sigma(t)| \leq M_\sigma$ for all t . Hence

$$\|\phi(x)\| \leq \sqrt{C} M_\sigma \quad \forall x \in K.$$

where, we recall, C stands for the number of imposed constraints. Therefore

$$\sup_{x \in K} \|U(x)\| = \sup_{x \in K} \|A_1 \phi(x)\| \leq \|A_1\| \sup_{x \in K} \|\phi(x)\| \leq \|A_1\| \sqrt{C} M_\sigma.$$

Using $A_1 = R(M^\top)^{-1}$,

$$\|A_1\| \leq \|R\| \|(M^\top)^{-1}\|.$$

Moreover, since each column of R is r_l with $\|r_l\| < \delta$, we have $\|R\| \leq \sqrt{C} \delta$ (e.g. by Frobenius norm bound). Thus

$$\sup_{x \in K} \|U(x)\| \leq (\sqrt{C} \delta) \|(M^\top)^{-1}\| (\sqrt{C} M_\sigma) = C M_\sigma \|(M^\top)^{-1}\| \delta.$$

Putting the two terms together:

$$\sup_{x \in K} \|F(x) - H(x)\| < \delta + C M_\sigma \|(M^\top)^{-1}\| \delta = \delta \left(1 + C M_\sigma \|(M^\top)^{-1}\|\right).$$

Choose

$$\delta := \frac{\varepsilon}{1 + C M_\sigma \|(M^\top)^{-1}\|}.$$

Then $\sup_{x \in K} \|F(x) - H(x)\| < \varepsilon$.

Thus $H \in \mathcal{N}_{m,0}$ approximates $F \in \mathcal{F}_0$ arbitrarily well while matching the fixed points exactly. \square

After proving that the fixed-point constraints $F_\theta(\bar{x}^{(l)}) = 0$, $l = 1, \dots, C$ do not hinder universality, we note that a trivial corollary of the abovementioned proof is the fact that any set of local constraints of the form

$$F_\theta(\bar{x}^{(l)}) = c^{(l)}, \quad l = 1, \dots, C \tag{3}$$

still obeys the same universality theorem by generalizing the residuals to $r_l = -G(\bar{x}^{(l)}) + c^{(l)}$.

4 Planting fixed-points in Neural-ODEs

The universality theorem proved above is an *existence* result. Stated differently, it guarantees that the constrained class $\mathcal{N}_{m,0} = \{F_\theta \in \mathcal{N}_m : F_\theta(\bar{x}^{(l)}) = 0, l = 1, \dots, C\}$ is dense in the class of compatible vector fields. In this Section, we provide an operative perspective, by elaborating on a *constructive and training-friendly* recipe to impose the fixed-point $F_\theta(\bar{x}^{(l)}) = 0$ within a Neural-ODE, so that gradient-based training cannot drift outside the constrained class (namely the class that accommodates for the fixed points constraints).

4.1 Neural-ODE parametrization

We hereafter consider a slightly modified version of the Neural-ODE velocity field as discussed above. More specifically, we set:

$$\dot{x}(t) = F_\theta(x(t)), \quad F_\theta(x) := -x + A_1 f(A_2 x + b_2) + b_1, \tag{4}$$

where $x(t) \in \mathbb{R}^n$, $A_2 \in \mathbb{R}^{m \times n}$, $b_2 \in \mathbb{R}^m$, $A_1 \in \mathbb{R}^{n \times m}$, $b_1 \in \mathbb{R}^n$, and $f : \mathbb{R}^m \rightarrow \mathbb{R}^m$ is applied component-wise (e.g. $f(z)_j = \sigma(z_j)$).

Although Theorem 1 is stated for vector fields of the form $Af(Bx + b)$, the same construction applies to the residual parametrization

$$F_\theta(x) = -x + A_1 f(A_2 x + b_2) + b_1.$$

Indeed, for a target field F with prescribed equilibria $F(\bar{x}^{(l)}) = 0$, it is enough to consider the shifted field

$$\tilde{F}(x) = F(x) + x - b_1.$$

Hence the universality result carries over to the residual model used in the numerical experiments. We used this modified model as it can be mapped, in some suitable limit, to a coupled multi-population dynamical system, in the spirit of the Funahashi–Nakamura construction ichi Funahashi and Nakamura [1993]. As we plan to use this constrained Neural-ODE model in future works to investigate some biologically inspired models rooted in neuroscience, we opted to investigate this slight modification without loss of generality.

Notice that in the right-hand side of (4) we have subtracted a linear term ($-x$) without loss of generality. For the sake of completeness, we now apply biases on both layers, via b_1 and b_2 . Given C desired equilibria, $\{\bar{x}^{(l)}\}_{l=1}^C \subset \mathbb{R}^n$, the fixed-point constraints are

$$F_\theta(\bar{x}^{(l)}) = 0, \quad l = 1, \dots, C. \quad (5)$$

Evaluating (4) at $\bar{x}^{(l)}$ gives

$$0 = -\bar{x}^{(l)} + A_1 f(A_2 \bar{x}^{(l)} + b_2) + b_1 \iff A_1 s_l = y_l,$$

where we define the *feature vectors* and *targets* as, respectively:

$$s_l := f(A_2 \bar{x}^{(l)} + b_2) \in \mathbb{R}^m, \quad y_l := \bar{x}^{(l)} - b_1 \in \mathbb{R}^n. \quad (6)$$

Stack these quantities into matrices

$$S := [s_1, \dots, s_C] \in \mathbb{R}^{m \times C}, \quad Y := [y_1, \dots, y_C] \in \mathbb{R}^{n \times C}. \quad (7)$$

Then the C fixed-point constraints (5) are equivalent to the single matrix equation

$$A_1 S = Y. \quad (8)$$

As a key observation, for fixed (A_2, b_2, b_1) , the constraint (8) is *linear* in A_1 .

4.2 Pseudoinverse-based planting

Assume that the planted features are linearly independent, i.e.

$$\text{rank}(S) = C, \quad \text{in particular } m > C. \quad (9)$$

Under (9), the linear system (8) is solvable and has infinitely many solutions. A canonical choice is the minimum-norm solution obtained via the Moore–Penrose pseudoinverse S^+ :

$$A_{\text{part}} := Y S^+ \implies A_{\text{part}} S = Y. \quad (10)$$

To preserve full freedom (for training purposes) while adjusting for the sought constraints, we proceed as follows. Let

$$P := S S^+ \in \mathbb{R}^{m \times m}, \quad (11)$$

which is the (orthogonal) projector onto $\text{span}(S)$. Since each column of S lies in $\text{span}(S)$, we have

$$(I - P)S = 0. \quad (12)$$

Therefore, for any free matrix $W \in \mathbb{R}^{n \times m}$ we can define

$$A_1 := A_{\text{part}} + W(I - P), \quad (13)$$

and automatically obtain

$$A_1 S = A_{\text{part}} S + W(I - P)S = Y + W \cdot 0 = Y.$$

Hence (8) holds exactly, and consequently $F_\theta(\bar{x}^{(l)}) = 0$ for all l . Importantly, the constraints are satisfied *for all values of the free parameters* W . Hence, and as already remarked, training cannot drift outside the constrained class.

Remark (computational issue). While (13) is conceptually clean, computing S^+ via an SVD-based pseudoinverse can be computationally expensive and hide numerical pitfalls when S is ill-conditioned (especially as C grows). Next, we show how to obtain the *same* constrained matrix A_1 via a QR factorization, which replaces the pseudoinverses by stable triangular solves.

4.3 QR-based planting

Assume again (9). Consider a thin QR decomposition Golub and Loan [2013], Ben-Israel and Greville [2003] of the feature matrix:

$$S = QR, \quad (14)$$

where $Q \in \mathbb{R}^{m \times C}$ has orthonormal columns ($Q^\top Q = I_C$) and $R \in \mathbb{R}^{C \times C}$ is upper triangular and invertible. Since $\text{span}(S) = \text{span}(Q)$, the orthogonal projector onto $\text{span}(S)$ is

$$P = QQ^\top, \quad (15)$$

and again $(I - P)S = 0$ because each column of S lies in $\text{span}(Q)$.

We have to find now a particular solution via QR. We want $A_{\text{part}}S = Y$. Using $S = QR$, this is

$$A_{\text{part}}QR = Y.$$

Define $B := A_{\text{part}}Q \in \mathbb{R}^{n \times C}$. Then the equation becomes

$$BR = Y. \quad (16)$$

Because R is upper triangular and invertible, (16) has the unique solution $B = YR^{-1}$, hence

$$A_{\text{part}} = BQ^\top = (YR^{-1})Q^\top. \quad (17)$$

In the numerical implementations it is not needed to form R^{-1} explicitly: one solves the triangular system $BR = Y$ by back-substitution (a stable $O(C^2)$ operation per output dimension).

By adding now the free nullspace component, as in the pseudoinverse case, we define the full family of solutions by adding a term that annihilates S :

$$A_1 := A_{\text{part}} + W(I - P) = (YR^{-1}Q^\top) + W(I - QQ^\top), \quad W \in \mathbb{R}^{n \times m} \text{ free.} \quad (18)$$

Then

$$A_1S = A_{\text{part}}S + W(I - P)S = Y + W \cdot 0 = Y,$$

so the constraints (8) (equivalently (5)) hold exactly.

In conclusion, the pseudoinverse and QR constructions enforce the *same* fixed-point constraints. The QR version should be preferred in practice because it avoids SVD-based pseudoinverses and replaces matrix inversion by triangular solves on R , which are typically more stable and faster Golub and Loan [2013], Ben-Israel and Greville [2003]. Moreover, the decomposition $A_1 = A_{\text{part}} + W(I - P)$ makes explicit that the constraints fix only the action of A_1 on $\text{span}(S)$, while leaving the orthogonal complement free for learning task-specific dynamics; hence, throughout training, the model is updated within the constrained class, while retaining substantial expressive freedom. If $\text{rank}(S) < C$ at some iterate, the constraints (8) may become incompatible (or redundant). In practice, one can (i) choose $m \geq C$, (ii) initialize so that S has full column rank, and (iii) add a mild conditioning regularizer that discourages collapse of the columns of S .

In the following Section, we will turn to perform a set of numerical experiments that are aimed at testing the ability of the scheme to reproduce the velocity field of paradigmatic dynamical systems, with (stable or unstable) fixed points. These tests constitute the first validation of the proposed model.

5 Numerical experiments: vector-field regression with planted fixed points

This section empirically reports the ability of the proposed scheme to handle regression of a target velocity field which displays a collection of (stable or unstable) fixed points. In turn, this is aimed at providing a (non exhaustive) numerical validation, for the proof of universality as reported in Section 2. More concretely, we will consider supervised *vector-field regression* on a compact domain: given a target velocity field $F_* : K \rightarrow \mathbb{R}^2$ and pointwise samples $\{(x_i, F_*(x_i))\}$, we shall train a one-hidden-layer Neural-ODE vector field F_θ to approximate F_* while exactly accommodating for the fixed point gathered from the target velocity field F_* . The fixed-point constraints are imposed *by construction* through the QR-based planting parametrization described in Section 4.3, so that gradient-based optimization cannot drift outside the constrained hypothesis class.

5.1 Constrained approximation model

Given a target field F_\star on a compact set $K \subset \mathbb{R}^2$, we minimize the mean-squared regression loss (seeB)

$$\mathcal{L}(\theta) = \frac{1}{N_{\text{train}}} \sum_{i=1}^{N_{\text{train}}} \|F_\theta(x_i) - F_\star(x_i)\|_2^2, \quad (19)$$

using samples x_i drawn uniformly in K . To check that the constraints are correctly accommodated for, we monitor the fixed-point residual

$$r_{\text{fp}}(\theta) := \max_{l=1, \dots, C} \|F_\theta(\bar{x}^{(l)})\|_2, \quad (20)$$

which should remain at (numerical) round-off level (since the constraints are imposed by construction). To assess spatial accuracy, we also evaluate the pointwise error on a dense grid,

$$e(x) := \|F_\theta(x) - F_\star(x)\|_2, \quad (21)$$

and visualize $e(x)$ as a log-scale heatmap.

5.2 Experiment 1: generalized Lotka-Volterra vector field with resources competition

Let $K = [-1, 4] \times [-1, 4] \subset \mathbb{R}^2$ and define the polynomial target vector field $F_{\text{base}} : \mathbb{R}^2 \rightarrow \mathbb{R}^2$ by

$$F_{\text{base}}(x, y) = \begin{pmatrix} x(3 - x) - 2xy \\ y(2 - y) - xy \end{pmatrix}. \quad (22)$$

This is a specific realization of the celebrated Lotka-Volterra competition model, a foundational mathematical framework in ecology. The model is often invoked to predict the outcomes of the inter-species competition under limited resources. It directly supports the principle of competitive exclusion (Gauss’s Law), which states that two species competing for the same resource cannot stably coexist, if all other ecological factors stay constant.

The specific field defined by Eqs. (22) admits four equilibria inside K , namely $\bar{x}^{(1)} = (0, 0)$, $\bar{x}^{(2)} = (0, 2)$, $\bar{x}^{(3)} = (3, 0)$ and $\bar{x}^{(4)} = (1, 1)$. It is straightforward to verify by direct inspection that $F_{\text{base}}(\bar{x}^{(l)}) = 0$, for all $l = 1, \dots, 4$. We set $C = 4$ and plant exactly these equilibria via (2). We sample $N_{\text{train}} = 10^6$ points uniformly in K and minimize (19) with Adam Kingma and Ba [2014] (learning rate 10^{-3}) using mini-batches of size 500. At each optimization step we recompute A_1 using (26), ensuring the constraints remain satisfied throughout training. Figure 2 reports on the qualitative comparison between the target phase portrait and the learned constrained phase portrait, together with the spatial distribution of the error $e(x)$.

To quantify the variability due to random initialization, data sampling, and stochastic mini-batch optimization, we repeat the experiment over 10 independent random seeds and report mean \pm standard deviation. All runs were performed using PyTorch on a NVIDIA RTX A5500 with Data Loaders `num_workers=4`. The mean wall-clock time per training run was 3.99 ± 0.02 minutes over the 10 seeds. Figure 2 shows the qualitative comparison between the target phase portrait and the learned constrained phase portrait, together with the spatial distribution of the error $e(x)$. The constrained model accurately recovers the global structure of F_{base} on K while preserving the prescribed equilibria. Quantitatively, we report a grid MSE of $7.48 \times 10^{-5} \pm 1.72 \times 10^{-4}$, a grid RMSE of $6.28 \times 10^{-3} \pm 6.27 \times 10^{-3}$, and a maximum pointwise error of $1.05 \times 10^{-1} \pm 9.25 \times 10^{-2}$. The fixed-point residual remains small across runs, with value $2.31 \times 10^{-5} \pm 1.60 \times 10^{-5}$, confirming that the QR-planted parametrization prevents drift away from the prescribed hard constraints while retaining enough flexibility to fit the target vector field.

Another experiment of regression of a dynamical system involving a limit cycle behaviour is reported in C.

The code is available on Github.

6 Conclusions

In this work we addressed a basic question for constrained Neural-ODE models: can one impose a finite set of exact equilibrium conditions without sacrificing approximation power? The answer is

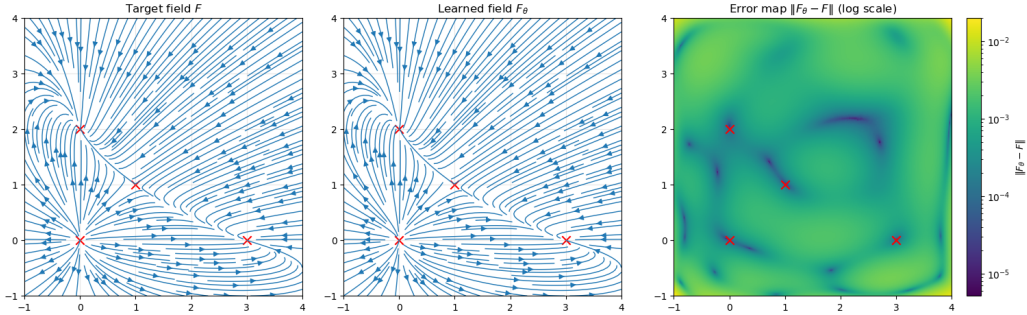


Figure 2: Vector-field regression with four planted fixed points. (Left) Target field F_{base} from (22). (Center) Learned constrained field F_{θ} from (25)–(26). (Right) Log-scale error heatmap $e(x) = \|F_{\theta}(x) - F_{\text{base}}(x)\|_2$. Red crosses indicate the prescribed equilibria, which are matched (up to numerical precision) by construction.

affirmative. Indeed, we proved that, on compact sets, the subclass of models satisfying prescribed fixed-point constraints remains dense in the class of continuous target vector fields that are compatible with those constraints. In this sense, planting equilibria does not reduce expressivity within the admissible hypothesis class.

We then turned this existence result into a practical parametrization for training. For the residual Neural-ODE architecture studied in the paper, the fixed-point conditions can be rewritten as a linear system for the output matrix. This yields a family of exact constrained parametrizations, which we expressed in two equivalent ways: through the Moore-Penrose pseudoinverse and through a thin QR factorization. The QR formulation is especially convenient in practice, because it avoids explicit pseudoinverses. Further, it makes clear how the constrained solution decomposes into a particular component that enforces the prescribed equilibria and a free relic that remains available for learning the suited residual dynamics. As a consequence, gradient-based optimization evolves entirely within the constrained model class, with no penalty terms and no post-training projection.

The numerical experiments support this picture. In the competition-model example, the constrained Neural-ODE accurately reproduces the target vector field while matching all four prescribed equilibria exactly. In the oscillatory glycolysis-inspired example, the same construction preserves the imposed equilibrium and still captures the surrounding phase-portrait geometry, including the regime associated with a stable periodic orbit. Taken together, these tests show that hard equilibrium constraints can be incorporated into Neural-ODE vector-field regression without preventing accurate approximation of qualitatively different dynamics.

We conclude by remarking that the present work focuses only on the exact placement of equilibria. It does not, by itself, enforce their stability or control the local Jacobian structure. Extending the construction so as to constrain not only the fixed points location but also their stability class, basin geometry, or other invariant features is therefore a natural next step. Further relevant directions include a systematic conditioning analysis of the constrained parametrization and other applications to data-driven dynamical systems in which part of the equilibrium structure is known a priori.

Broader impacts. This work contributes a constrained parametrization for Neural ODEs that allows prescribed fixed points to be enforced exactly. A positive potential impact is improved reliability and interpretability of learned dynamical systems, especially in scientific and engineering settings where known equilibria should be preserved by construction. Such constraints may reduce physically or mathematically inconsistent predictions and can make learned models easier to validate against prior domain knowledge.

References

- Ricky T. Q. Chen, Yulia Rubanova, Jesse Bettencourt, and David Duvenaud. Neural ordinary differential equations. In *Advances in Neural Information Processing Systems (NeurIPS)*, 2018. arXiv:1806.07366.
- Takeshi Teshima, Koichi Tojo, Masahiro Ikeda, Isao Ishikawa, and Kenta Oono. Universal approximation property of neural ordinary differential equations. *arXiv preprint arXiv:2012.02414*, 2020.
- Isao Ishikawa, Takeshi Teshima, Koichi Tojo, Kenta Oono, Masahiro Ikeda, and Masashi Sugiyama. Universal approximation property of invertible neural networks. *Journal of Machine Learning Research*, 24(287):1–68, 2023.
- Youngjae Min and Navid Azizan. Hardnet: Hard-constrained neural networks with universal approximation guarantees. *arXiv preprint arXiv:2410.10807*, 2024.
- Feilong Cao, Shaobo Lin, and Zongben Xu. Approximation capability of interpolation neural networks. *Neurocomputing*, 74(1):457–460, 2010. ISSN 0925-2312. doi: <https://doi.org/10.1016/j.neucom.2010.08.018>. URL <https://www.sciencedirect.com/science/article/pii/S0925231210003978>. Artificial Brains.
- Isaac E Lagaris, Aristidis Likas, and Dimitrios I Fotiadis. Artificial neural networks for solving ordinary and partial differential equations. *IEEE transactions on neural networks*, 9(5):987–1000, 1998.
- Hao Chen, Gonzalo E Constante Flores, and Can Li. Physics-informed neural networks with hard linear equality constraints. *Computers & Chemical Engineering*, 189:108764, 2024.
- Natarajan Sukumar and Ankit Srivastava. Exact imposition of boundary conditions with distance functions in physics-informed deep neural networks. *Computer Methods in Applied Mechanics and Engineering*, 389:114333, 2022.
- Vlad-Raul Constantinescu and Ionel Popescu. Approximation and interpolation of deep neural networks. *arXiv preprint arXiv:2304.10552*, 2023.
- Karthik Elamvazhuthi, Xuechen Zhang, Samet Oymak, and Fabio Pasqualetti. Learning on manifolds: Universal approximations properties using geometric controllability conditions for neural odes. In *Learning for Dynamics and Control Conference*, pages 1–11. PMLR, 2023.
- Qiyu Kang, Yang Song, Qinxu Ding, and Wee Peng Tay. Stable neural ode with lyapunov-stable equilibrium points for defending against adversarial attacks. *Advances in Neural Information Processing Systems*, 34:14925–14937, 2021.
- Brandon Amos and J Zico Kolter. Optnet: Differentiable optimization as a layer in neural networks. In *International conference on machine learning*, pages 136–145. PMLR, 2017.
- Stefano Gagliani, Feliciano Giuseppe Pacifico, Lorenzo Chicchi, Duccio Fanelli, Diego Febbe, Lorenzo Buffoni, and Raffaele Marino. Train stochastic non linear coupled odes to classify and generate. *Machine Learning: Science and Technology*, 7:025020, 2026. doi: 10.1088/2632-2153/ae493a.
- Lorenzo Chicchi, Duccio Fanelli, Diego Febbe, Lorenzo Buffoni, Francesca Di Patti, Lorenzo Giambagli, and Raffaele Marino. Deterministic versus stochastic dynamical classifiers: opposing random adversarial attacks with noise. *Machine Learning: Science and Technology*, 6(3):035054, sep 2025. doi: 10.1088/2632-2153/ae0244. URL <https://doi.org/10.1088/2632-2153/ae0244>.
- Alistair White, Anna Büttner, Maximilian Gelbrecht, Valentin Duruisseaux, Niki Kilbertus, Frank Hellmann, and Niklas Boers. Projected neural differential equations for learning constrained dynamics. *arXiv preprint arXiv:2410.23667*, 2024.

- Kurt Hornik, Maxwell Stinchcombe, and Halbert White. Multilayer feedforward networks are universal approximators. *Neural Networks*, 2(5):359–366, 1989. ISSN 0893-6080. doi: [https://doi.org/10.1016/0893-6080\(89\)90020-8](https://doi.org/10.1016/0893-6080(89)90020-8). URL <https://www.sciencedirect.com/science/article/pii/0893608089900208>.
- G Cybenko. Approximation by superpositions of a sigmoidal function. *Mathematics of Control, Signal and Systems*, 2:303–314, 1989.
- Ken ichi Funahashi and Yuichi Nakamura. Approximation of dynamical systems by continuous time recurrent neural networks. *Neural Networks*, 6(6):801–806, 1993. ISSN 0893-6080. doi: [https://doi.org/10.1016/S0893-6080\(05\)80125-X](https://doi.org/10.1016/S0893-6080(05)80125-X). URL <https://www.sciencedirect.com/science/article/pii/S089360800580125X>.
- Gene H. Golub and Charles F. Van Loan. *Matrix Computations*. Johns Hopkins University Press, Baltimore, 4 edition, 2013.
- Adi Ben-Israel and Thomas N. E. Greville. *Generalized Inverses: Theory and Applications*. Springer, New York, 2 edition, 2003. doi: 10.1007/b97366.
- Diederik P Kingma and Jimmy Ba. Adam: A method for stochastic optimization. *arXiv preprint arXiv:1412.6980*, 2014.

A On the existence of the inverse of matrix M

In the above proof we assumed that it is always possible to choose the weights W and the bias β so to have matrix M invertible. Here we provide a proof of the assumption.

Lemma 2. *Let $\bar{x}^{(1)}, \dots, \bar{x}^{(C)} \in \mathbb{R}^n$ be C distinct points and let $\sigma : \mathbb{R} \rightarrow \mathbb{R}$ be continuous with two distinct one-sided limits (This holds, for instance, for tanh and sigmoid activations.)*

$$\alpha := \lim_{t \rightarrow -\infty} \sigma(t), \quad \beta := \lim_{t \rightarrow +\infty} \sigma(t), \quad \alpha \neq \beta.$$

Then there exist parameters $(w_k, \beta_k)_{k=1}^C \subset \mathbb{R}^n \times \mathbb{R}$ such that the matrix

$$M \in \mathbb{R}^{C \times C}, \quad M_{lk} = \sigma(w_k^\top \bar{x}^{(l)} + \beta_k),$$

is invertible.

Proof.

Choose a projection that separates the points:

We want to find a direction $a \in \mathbb{R}^n$ such that the one-dimensional projections

$$t_l := a^\top \bar{x}^{(l)}, \quad l = 1, \dots, C,$$

are all distinct. Notice that two projections collide, i.e. $t_l = t_m$, if and only if

$$a^\top \bar{x}^{(l)} = a^\top \bar{x}^{(m)} \iff a^\top (\bar{x}^{(l)} - \bar{x}^{(m)}) = 0.$$

Fix a pair $l \neq m$ and denote $d_{lm} := \bar{x}^{(l)} - \bar{x}^{(m)} \neq 0$ (since the points are distinct). The set of directions a for which the projections of $\bar{x}^{(l)}$ and $\bar{x}^{(m)}$ coincide is therefore

$$H_{lm} := \{a \in \mathbb{R}^n : a^\top d_{lm} = 0\}.$$

Geometrically, H_{lm} is the set of all vectors a orthogonal to d_{lm} , hence it is an $(n-1)$ -dimensional hyperplane (a codimension-1 linear subspace) in \mathbb{R}^n .

The number of pairs (l, m) is finite and total in $\binom{C}{2}$. Hence, the number of unsuitable hyperplanes (those that yield coinciding projections) is finite.

A finite union of hyperplanes cannot cover the whole space \mathbb{R}^n (hyperplanes have codimension 1 and thus cannot fill an open set). Consequently, we can choose a direction

$$a \in \mathbb{R}^n \setminus \bigcup_{l < m} H_{lm},$$

which implies $a^\top (\bar{x}^{(l)} - \bar{x}^{(m)}) \neq 0$ for all $l \neq m$, i.e. $t_l \neq t_m$ for all $l \neq m$.

Define $t_l := a^\top \bar{x}^{(l)}$ and relabel the points so that

$$t_1 < t_2 < \dots < t_C.$$

Define a “staircase” target matrix:

Using the constants α, β introduced in the statement of the lemma, we define the staircase $C \times C$ matrix M_\star by

$$(M_\star)_{lk} := \begin{cases} \alpha, & l < k, \\ \beta, & l \geq k. \end{cases} \quad (23)$$

Written out, M_\star has the “staircase” form depicted in the following

$$M_\star = \begin{pmatrix} \beta & \alpha & \alpha & \cdots & \alpha \\ \beta & \beta & \alpha & \cdots & \alpha \\ \beta & \beta & \beta & \cdots & \alpha \\ \vdots & \vdots & \vdots & \ddots & \vdots \\ \beta & \beta & \beta & \cdots & \beta \end{pmatrix}.$$

Compute $\det(M_\star)$:

Perform the following determinant-preserving row operations: for $i = 1, \dots, C-1$, replace row $(i+1)$ by row $(i+1)$ minus row i . Denote the resulting matrix by \widetilde{M}_\star . Let us inspect the new rows.

For $i = 1$, row 2 minus row 1 gives

$$(\beta - \beta, \beta - \alpha, \alpha - \alpha, \dots, \alpha - \alpha) = (0, \beta - \alpha, 0, \dots, 0).$$

For $i = 2$, row 3 minus row 2 gives

$$(\beta - \beta, \beta - \beta, \beta - \alpha, \alpha - \alpha, \dots, \alpha - \alpha) = (0, 0, \beta - \alpha, 0, \dots, 0),$$

and so on. In general, for $i = 1, \dots, C-1$ the row difference $(i+1) - i$ produces a row which is zero everywhere except at column $(i+1)$, where it equals $\beta - \alpha$. Therefore \widetilde{M}_\star is lower triangular and has diagonal entries

$$\widetilde{M}_{\star,11} = \beta, \quad \widetilde{M}_{\star,22} = \beta - \alpha, \quad \widetilde{M}_{\star,33} = \beta - \alpha, \dots, \quad \widetilde{M}_{\star,CC} = \beta - \alpha.$$

$$\widetilde{M}_\star = \begin{pmatrix} \beta & \alpha & \alpha & \cdots & \alpha \\ 0 & \beta - \alpha & 0 & \cdots & 0 \\ 0 & 0 & \beta - \alpha & \cdots & 0 \\ \vdots & \vdots & \vdots & \ddots & \vdots \\ 0 & 0 & 0 & \cdots & \beta - \alpha \end{pmatrix}.$$

Hence

$$\det(M_\star) = \det(\widetilde{M}_\star) = \beta(\beta - \alpha)^{C-1}. \quad (24)$$

Since $\alpha \neq \beta$ (by sigmoidal activation function assumption), we have $\beta - \alpha \neq 0$; Thus $\det(M_\star) \neq 0$, so M_\star is invertible. If $\beta \neq 0$, then

$$\det(M^\star) = \beta(\beta - \alpha)^{C-1} \neq 0.$$

If instead $\beta = 0$, then necessarily $\alpha \neq 0$ since $\alpha \neq \beta$. In this case, one simply exchanges the roles of α and β in the construction of M^\star ; the same row-operation argument then gives

$$\det(M^\star) = \alpha(\alpha - \beta)^{C-1} \neq 0.$$

Therefore, in both cases, the matrix M^\star is invertible.

Make M arbitrarily close to M_\star with suitable neurons:

Choose thresholds θ_k such that

$$t_{k-1} < \theta_k < t_k, \quad k = 1, \dots, C,$$

with the convention $t_0 := -\infty$ so that $\theta_1 < t_1$. For a gain parameter $\lambda > 0$, define

$$w_k := \lambda a, \quad \beta_k := -\lambda \theta_k, \quad \phi_k(x) := \sigma(w_k^\top x + \beta_k) = \sigma(\lambda(a^\top x - \theta_k)).$$

Then for each fixed point $\bar{x}^{(l)}$ we have

$$\phi_k(\bar{x}^{(l)}) = \sigma(\lambda(t_l - \theta_k)).$$

By construction, if $l < k$ then $t_l < \theta_k$ so $t_l - \theta_k < 0$; if $l \geq k$ then $t_l > \theta_k$ so $t_l - \theta_k > 0$. Hence, as λ increases, the arguments $\lambda(t_l - \theta_k)$ become large negative for $l < k$ and large positive for $l \geq k$. Because σ is continuous and non-constant, and since α and β are distinct values of the image of the non linear function σ , one can set λ large enough so that

$$|\sigma(\lambda(t_l - \theta_k)) - \alpha| < \eta \quad \text{for } l < k, \quad |\sigma(\lambda(t_l - \theta_k)) - \beta| < \eta \quad \text{for } l \geq k,$$

for any prescribed $\eta > 0$. Equivalently, $M(\lambda)_{lk} := \phi_k(\bar{x}^{(l)}) = \sigma(\lambda(t_l - \theta_k))$, yields $M(\lambda) \rightarrow M_\star$ entrywise as $\lambda \rightarrow \infty$.

Conclude on the invertibility of M by continuity of the determinant:

The determinant is a continuous function of the matrix entries. Since $M(\lambda) \rightarrow M_\star$ and $\det(M_\star) \neq 0$ by (24), there exists λ_0 such that for all $\lambda \geq \lambda_0$,

$$\det(M(\lambda)) \neq 0.$$

In particular, by choosing $\lambda \geq \lambda_0$ yields an invertible evaluation matrix M . This completes the proof. \square

B Details for numerical experiments

Throughout this section we use the residual one-hidden-layer parametrization introduced in Section 4, as the Neural-ODE regressor. In formulae:

$$F_\theta(x) = -x + A_1 f(A_2 x + b_2) + b_1, \quad (25)$$

where $x \in \mathbb{R}^2$, $A_2 \in \mathbb{R}^{m \times 2}$, $b_2 \in \mathbb{R}^m$, $A_1 \in \mathbb{R}^{2 \times m}$, $b_1 \in \mathbb{R}^2$, and f is applied componentwise (sigmoid in the experiments below). We fix the hidden width to $m = 256$.

Given the prescribed equilibria $\{\bar{x}^{(l)}\}_{l=1}^C \subset K$ we enforce $F_\theta(\bar{x}^{(l)}) = 0$.

As shown in Section 4, these constraints are equivalent to solving the linear system $A_1 S = Y$, where the feature matrix $S \in \mathbb{R}^{m \times C}$ and the target matrix $Y \in \mathbb{R}^{2 \times C}$ are defined by

$$s_l := f(A_2 \bar{x}^{(l)} + b_2), \quad S := [s_1, \dots, s_C], \quad Y := [\bar{x}^{(1)} - b_1, \dots, \bar{x}^{(C)} - b_1].$$

Assuming $\text{rank}(S) = C$ (generically satisfied when $m \gg C$), we compute a thin QR factorization

$$S = QR,$$

with $Q \in \mathbb{R}^{m \times C}$ having orthonormal columns and $R \in \mathbb{R}^{C \times C}$ upper triangular and invertible. We then set

$$A_1 = (Y R^{-1} Q^\top) + W(I - Q Q^\top), \quad (26)$$

where $W \in \mathbb{R}^{2 \times m}$ is a free matrix trained by gradient descent (together with A_2, b_2, b_1). In practice, R^{-1} is never formed explicitly: the factor $Y R^{-1}$ is obtained by solving the triangular system $B R = Y$ for B .

By construction, (26) implies $A_1 S = Y$ and therefore (2) holds for *all* values of the free parameters. This is the key practical feature of the planting mechanism: the optimization is always constrained to the subset of all possible vector fields that match the prescribed equilibria exactly, with no penalty terms and no post-hoc projection steps.

C Experiment 2: limit-cycle system with a planted equilibrium

We now test the same constrained parametrization on a qualitatively different phase portrait: a system with a single prescribed (unstable) fixed point and a stable periodic orbit. This experiment is meant to probe whether hard equilibrium constraints interfere with learning *non-equilibrium* fixed-points (here, a limit cycle). In particular, the planted constraint fixes the behavior at one point in state space, but leaves the remaining degrees of freedom available to approximate the global geometry of the flow, including periodic behavior.

Let $K = [-1, 4] \times [-1, 4] \subset \mathbb{R}^2$ and consider the (Brusselator-like) target vector field $F_{lc} : \mathbb{R}^2 \rightarrow \mathbb{R}^2$ defined by

$$F_{lc}(x, y) = \begin{pmatrix} -x + a y + x^2 y \\ b - a y - x^2 y \end{pmatrix}, \quad (a > 0, b > 0). \quad (27)$$

In the experiment we fix

$$a = 0.06, \quad b = 0.6.$$

Specifically the above system has been invoked as a minimal descriptive model of the glycolysis, a fundamental biochemical process by which living cells extract energy from sugar. Here x and y are the concentration of the ADP (adenosine diphosphate) and F6P (fructose-6-phosphate), respectively. A direct computation shows that F_{lc} has a unique equilibrium point

$$\bar{x}^{(1)} = \left(b, \frac{b}{a + b^2} \right), \quad (28)$$

and $F_{lc}(\bar{x}^{(1)}) = 0$. For the operated choice of parameters, the above fixed point is an unstable spiral. For this parameters' regime, trajectories from a broad set of initial conditions in K convergence spiraling toward a stable periodic orbit, yielding a limit-cycle phase portrait.

We approximate F_{lc} on K with the same constrained Neural-ODE model (25) (with $m = 256$). Here we set $C = 1$ and plant the equilibrium (28) by enforcing

$$F_\theta(\bar{x}^{(1)}) = 0, \quad (29)$$

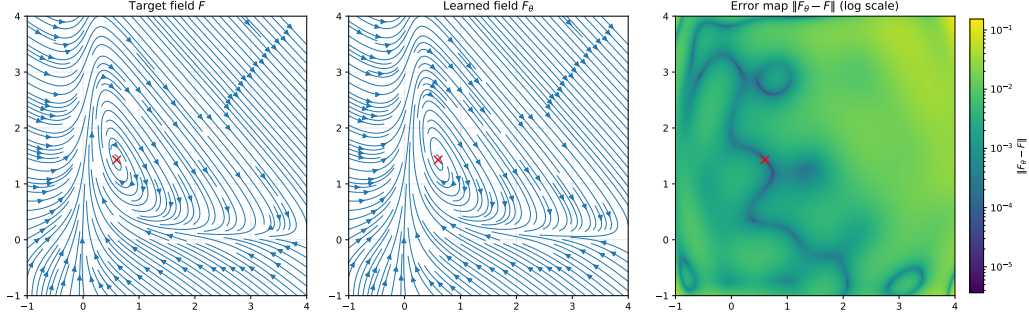


Figure 3: Vector-field regression for a limit-cycle system with a planted equilibrium. (*Left*) Target field F_{1c} from (27). (*Center*) Learned constrained field F_θ . (*Right*) Log-scale error heatmap $e(x) = \|F_\theta(x) - F_{1c}(x)\|_2$. The red cross marks the prescribed equilibrium (28), which is matched (up to numerical precision) by construction.

using the QR-based construction (26) (the case $C = 1$ reduces to a normalized one-dimensional projector, but the implementation is identical).

We sample $N_{\text{train}} = 10^6$ points uniformly in K and minimize the regression loss

$$\mathcal{L}(\theta) = \frac{1}{N_{\text{train}}} \sum_{i=1}^{N_{\text{train}}} \|F_\theta(x_i) - F_{1c}(x_i)\|_2^2, \quad (30)$$

training with Adam (learning rate 10^{-3}) and mini-batches of size 500 for 200 epochs. We monitor the planted-equilibrium residual

$$r_{\text{fp}}(\theta) := \|F_\theta(\bar{x}^{(1)})\|_2, \quad (31)$$

and visualize the log-scale pointwise error

$$e(x) := \|F_\theta(x) - F_{1c}(x)\|_2. \quad (32)$$

Figure 3 compares the target flow, the learned constrained approximation, and the resulting error heatmap. The learned field reproduces the qualitative geometry of the limit-cycle phase portrait on K , while the equilibrium constraint at $\bar{x}^{(1)}$ is preserved throughout training by construction (red cross). This confirms that imposing hard fixed-point constraints does not preclude approximating vector fields whose dominant fixed-point is a periodic orbit: the constraint fixes the flow at the planted equilibrium, but leaves enough expressivity to fit the surrounding dynamics.